



# Observationally constrained projection of the reduced intensification of extreme climate events in Central Asia from 0.5 °C less global warming

Dongdong Peng<sup>1,2,3</sup> · Tianjun Zhou<sup>2,3,4</sup> · Lixia Zhang<sup>2,4</sup> · Wenxia Zhang<sup>2</sup> · Xiaolong Chen<sup>2</sup>

Received: 2 January 2019 / Accepted: 10 October 2019 / Published online: 5 November 2019  
© The Author(s) 2019

## Abstract

Arid Central Asia is highly vulnerable to extreme climate events. Information on potential future changes in extreme climate events in Central Asia is limited. In this study, the performances of models from the Coupled Model Intercomparison Project phase 5 (CMIP5) in simulating climatological extremes in Central Asia are first evaluated, and a bias correction method is employed to constrain future projections. The responses of extreme climate events over Central Asia to future warming and, in particular, the impact of 1.5 and 2 °C global warming scenarios are then assessed based on the observationally constrained projections. During the twenty-first century, coldest night (TNn), coldest day (TXn), warmest night (TNx), warmest day (TXx), 1-day maximum precipitation (RX1 day), 5-day maximum precipitation (RX5 day), and precipitation intensity (SDII) in Central Asia would robustly increase at best estimated rates of 1.93 °C, 1.71 °C, 1.18 °C, 1.25 °C, 6.30%, 5.71%, and 4.99% per degree of global warming, respectively, under Representative Concentration Pathway (RCP) 8.5. Compared with the 2 °C warming scenario, limiting global warming to 1.5 °C could reduce the intensification (relative to 1986–2005) of TNn, TNx, TXn, TXx, RX1 day, RX5 day, and SDII by 33%, 24%, 32%, 29%, 39%, 42%, and 53% from the best estimates under RCP8.5, respectively. The avoided intensification of TNn, TNx, TXn and TXx (RX1 day and SDII) would be larger (smaller) under RCP4.5. This suggests that a low warming target is necessary for avoiding the dangerous risk of extremes in this arid region.

**Keywords** 1.5 and 2 °C · Central Asia · Extreme events

---

**Electronic supplementary material** The online version of this article (<https://doi.org/10.1007/s00382-019-05014-6>) contains supplementary material, which is available to authorized users.

---

✉ Tianjun Zhou  
zhoujt@lasg.iap.ac.cn

<sup>1</sup> Institute of Tropical and Marine Meteorology, China Meteorological Administration, Guangzhou, China

<sup>2</sup> LASG, Institute of Atmospheric Physics, Chinese Academy of Sciences, Beijing 100029, China

<sup>3</sup> University of Chinese Academy of Sciences, Beijing 100049, China

<sup>4</sup> CAS Center for Excellence in Tibetan Plateau Earth Sciences, Chinese Academy of Sciences (CAS), Beijing 100101, China

## 1 Introduction

Human-induced global warming has a great impact on society at both global and regional scales (IPCC 2013). Central Asia is an arid region with annual precipitation less than 300 mm and is characterized by a fragile ecological environment with sparse vegetation and vast barrenness (Huang et al. 2016; Hu et al. 2017). The ecosystem and societal development in this area are highly vulnerable to climate change (Huang et al. 2017). Understanding and projecting the potential changes in climate extremes over Central Asia are of great importance to both policymaking and climate change adaption activities.

Central Asia has witnessed significant warming during the past half-century at a rate of approximately 0.30 °C decade<sup>-1</sup>, which is much faster than the global land average rate (0.19 °C decade<sup>-1</sup>) (Hu et al. 2014; IPCC 2013). Associated with significant warming, precipitation in the eastern part of Central Asia has increased significantly in the

last five decades, demonstrating the shift in the climate from warm and dry to warm and wet (Shi et al. 2007; Zhao et al. 2014; Li et al. 2015; Peng and Zhou 2017). This wetting trend is largely influenced by the southward displacement of the Asian subtropical westerly jet and increased moisture and can be partly attributed to the human influence (Peng et al. 2018). Meanwhile, both extreme temperature and precipitation events in Central Asia have increased significantly during the past 50 years, while the dry lands have expanded (Jiang et al. 2013; Deng et al. 2014; Huang et al. 2015; Hu et al. 2016). However, how extreme climate events would change in this region in the future has not been investigated in detail thus far.

Previous analyses of future climate projections focused on Central Asia are rare in comparison to those focused on other parts of the world. The Intergovernmental Panel on Climate Change Fifth Assessment Report on Central Asia is mainly based on Coupled Model Intercomparison Project Phase 3 (CMIP3) models, which project a stronger than global mean warming trend in Central Asia for both winter and summer and the likely increase in mean precipitation (Christensen et al. 2013). Later analysis based on CMIP5 models further shows that the intensity, interannual variation, and long-term trend of annual mean precipitation in Central Asia during the twenty-first century would increase due to enhanced evaporation and increased precipitable water under different Representative Concentration Pathways (RCPs), with wetting centers in the northern, middle, and southeastern parts, respectively (Huang et al. 2014). In the eastern part of Central Asia, the projected cold events and consecutive dry days (warm events and wet days) would decrease (increase) significantly during the twenty-first century at a faster rate under higher RCPs (Wang et al. 2017). The accelerated expansion of dry lands in Central Asia would be seen in response to continued anthropogenic influence in the future (Huang et al. 2017).

To avoid the dangerous impact of anthropogenic climate change, the 2015 Paris Agreement, which was approved by a total of 175 parties (174 countries and the European Union) under the United Nations Framework Convention on Climate Change (UNFCCC), committed to “holding the increase in the global average temperature to well below 2 °C above preindustrial levels and pursuing efforts to limit the temperature increase to 1.5 °C above preindustrial levels” (UNFCCC 2015). Vulnerability in response to global warming is regionally dependent (Schleussner et al. 2016). Thus, climate changes in 1.5 and 2 °C warmer worlds (relative to the preindustrial level) have been assessed in specific regions in many recent studies (Dosio and Fischer 2017; King and Karoly 2017; King et al. 2017; Shi et al. 2018; Nangombe et al. 2018; Wang et al. 2018; Yang et al. 2018; Yu et al. 2018; Zhang et al. 2018; Zhou et al. 2018b, c). For example, under 1.5 and 2 °C global warming scenarios, more intense

and frequent extreme temperature events are projected for densely populated areas in China, Japan, and the Korean Peninsula (Li et al. 2018a; Shi et al. 2018; Yang et al. 2018), and this kind of change would impact many kinds of social activities, including air travel (Zhou et al. 2018a). Extreme precipitation events would be more intense under the 1.5 and 2 °C warming scenarios, and the events with longer return periods would increase (Li et al. 2018b, c). Some extreme temperature and precipitation events associated with high socially relevant impacts in eastern China are projected to increase significantly under 1.5 and 2 °C global warming scenarios (Lin et al. 2018).

In comparison to East Asia, less effort has been devoted to Central Asia. Although the changes in extreme events over Central Asia in 1.5 and 2 °C warmer worlds can be seen in some global studies (e.g., Schleussner et al. 2016; Wartenburger et al. 2017), information on corresponding changes in climate extremes in Central Asia remains unclear. Thus, the objective of this study is to assess the impact of 1.5 and 2 °C global warming scenarios on extreme events in Central Asia. Based on the CMIP5 models, we use eight extreme indices to quantify the projected changes. We show evidence that in comparison to the 2 °C warmer world, 0.5 °C less warming would result in a significant reduction in climate extremes in Central Asia, with intensification avoided by more than 24% for both temperature and precipitation extremes.

The remainder of this paper is organized as follows: the observations, model simulations and the definitions of extreme climate indices used in this study are described in Sect. 2. In Sect. 3, we first evaluate the performance of the CMIP5 models in simulating the historical extreme indices in Central Asia and then discuss the changes in extreme climate events in 1.5 and 2 °C warmer worlds based on the corrected projections. Finally, we summarize the main results in Sect. 4.

## 2 Data and methods

### 2.1 Data description

The following datasets are used in this study:

1. The global land-only gridded daily maximum and minimum temperature dataset HadGHCND, with a horizontal resolution of 3.75°/2.5° longitude/latitude covering the period from 1950 to present, is available at <https://www.metoffice.gov.uk/hadobs/hadghcnd/> (Caesar et al. 2006). The daily station minimum and maximum temperatures used in the HadGHCND dataset are mainly provided by the National Climatic Data Center (NCDC) Global Historical Climatology Network-Daily (GHCND). Please note that we do not use the HadEX2

- dataset here as observational evidence since the temperature extremes were calculated at points and then gridded, leading to scaling issues for the HadEX2 dataset (Caesar et al. 2006; Zhang et al. 2011; Donat et al. 2013; Sillmann et al. 2013; Dunn et al. 2014; Avila et al. 2015).
- The daily mean gridded precipitation from the Asian Precipitation Highly Resolved Observational Data Integration Towards Evaluation of Water Resources (APH-RODITE) project, version 1101, with a horizontal resolution of 0.5°/0.5° latitude/longitude covering the period from 1951 to 2007, is available from <http://www.chikyu.ac.jp/precip/english/products.html> (Yatagai et al. 2009, 2012). The dataset is maintained by the Research Institute for Humanity and Nature and the Meteorological Research Institute/Japan Meteorological Agency based on the rain gauge dataset from Asian countries.
  - The global gridded monthly mean air temperature Climate Research Unit (CRU) Time-Series Version 4.0, with a horizontal of 0.5°/0.5° longitude/latitude, covers the period from 1901 to 2015 (Harris and Jones 2017). This dataset is derived from the interpolation of global station data and has been widely used in previous studies to address temperature changes over Central Asia (Hu et al. 2014; Peng et al. 2019).
  - The outputs of historical simulations and future projections under RCP4.5 and RCP8.5 scenarios from 20 CMIP5 models are used in this study (Taylor et al. 2012). The studied variables are daily precipitation, maximum and minimum surface air temperatures, and monthly mean surface air temperature. All of the models that studied variables available from both historical and future projection experiments are selected. Only the first ensemble member (the first realization, initialization, and set of perturbed physics, which is denoted “r1i1p1”) from each experiment for the 20 CMIP5 models is used (Table 1). In total, 20 runs for each experiment are employed. Note that the multimodel ensemble mean (MME) of CMIP5 is calculated as the equal weighted average of all the available model runs. The convective schemes for the 20 employed models are illustrated in Table 2 and can be classified into 7 groups (“A”, “Be”, “Bo”, “D”, “G”, “T”, and “Z”).

## 2.2 Definitions of extreme indices and the skill score

In this study, we analyze four extreme temperature and precipitation indices from the Expert Team on Climate Change Detection and Indices (ETCCDI) to investigate the changes

**Table 1** The CMIP5 models used in this study and the timing of each model in reaching 1.5 °C and 2 °C global warming

Model name	Historical simulation	RCP4.5 simulation	RCP8.5 simulation	RCP4.5 1.5 (2.0) °C	RCP8.5 1.5 (2.0) °C
CanESM2	r1i1p1	r1i1p1	r1i1p1	2017 (2031)	2013 (2026)
CCSM4	r1i1p1	r1i1p1	r1i1p1	2017 (2040)	2014 (2030)
CMCC-CM	r1i1p1	r1i1p1	r1i1p1	2033 (2050)	2029 (2041)
CMCC-CMS	r1i1p1	r1i1p1	r1i1p1	2034 (2053)	2030 (2041)
CNRM-CM5	r1i1p1	r1i1p1	r1i1p1	2035 (2056)	2030 (2044)
CSIRO-Mk3-6-0	r1i1p1	r1i1p1	r1i1p1	2034 (2048)	2034 (2044)
FGOALS-g2	r1i1p1	r1i1p1	r1i1p1	2039 (—)	2030 (2046)
GFDL-ESM2G	r1i1p1	r1i1p1	r1i1p1	2051 (—)	2038 (2055)
GFDL-ESM2 M	r1i1p1	r1i1p1	r1i1p1	2045 (—)	2035 (2051)
HadGEM2-CC	r1i1p1	r1i1p1	r1i1p1	2038 (2055)	2029 (2041)
inmcm4	r1i1p1	r1i1p1	r1i1p1	2062 (—)	2045 (2058)
IPSL-CM5A-LR	r1i1p1	r1i1p1	r1i1p1	2015 (2031)	2012 (2027)
IPSL-CM5B-LR	r1i1p1	r1i1p1	r1i1p1	2027 (2050)	2023 (2038)
MIROC5	r1i1p1	r1i1p1	r1i1p1	2040 (2073)	2034 (2049)
MIROC-ESM-CHEM	r1i1p1	r1i1p1	r1i1p1	2022 (2035)	2018 (2030)
MIROC-ESM	r1i1p1	r1i1p1	r1i1p1	2021 (2034)	2021 (2030)
MPI-ESM-LR	r1i1p1	r1i1p1	r1i1p1	2021 (2042)	2017 (2036)
MPI-ESM-MR	r1i1p1	r1i1p1	r1i1p1	2024 (2046)	2020 (2039)
MRI-CGCM3	r1i1p1	r1i1p1	r1i1p1	2054 (2085)	2041 (2053)
NorESM1-M	r1i1p1	r1i1p1	r1i1p1	2041 (2074)	2034 (2050)
Total (20)	20	20	20	20 (16)	20 (20)

The symbol “—” indicates that the model-projected warming magnitude is less than 2 °C during the twenty-first century

**Table 2** Information on the convective schemes employed for the CMIP5 model in this study

Model name	Convective scheme	Classification
CanESM2	Zhang and McFarlane (1995)	Z
CCSM4	Zhang and McFarlane (1995)	Z
CMCC-CM	Tiedtke (1989)	T
CMCC-CMS	Tiedtke (1989)	T
CNRM-CM5	Bougeault (1985)	Bo
CSIRO-Mk3-6-0	Gregory and Rowntree (1990)	G
FGOALS-g2	Zhang and McFarlane (1995)	Z
GFDL-ESM2G	Donner (1993)	D
GFDL-ESM2M	Donner (1993)	D
HadGEM2-CC	Gregory and Rowntree (1990)	G
inmcm4	Betts (1986)	Be
IPSL-CM5A-LR	Tiedtke (1989), Emanuel (1991, 1993)	T
IPSL-CM5B-LR	Tiedtke (1989), Emanuel (1991, 1993)	T
MIROC5	Arakawa and Schubert (1974)	A
MIROC-ESM-CHEM	Arakawa and Schubert (1974)	A
MIROC-ESM	Arakawa and Schubert (1974)	A
MPI-ESM-LR	Tiedtke (1989)	T
MPI-ESM-MR	Tiedtke (1989)	T
MRI-CGCM3	Tiedtke (1989)	T
NorESM1-M	Zhang and McFarlane (1995)	Z

in extreme events in Central Asia (Zhang et al. 2011), as shown in Table 3. The four temperature extreme indices are the annual maximum (TXx) and minimum (TXn) of the daily maximum temperature and the annual maximum (TNx) and minimum (TNn) of the daily minimum temperature. The four precipitation extreme indices are the annual maximum length of consecutive dry days (CDD) with daily precipitation less than 1 mm, the maximums of 1-day (RX1 day) and 5-day (RX5 day) precipitation, and the simple precipitation intensity index (SDII) averaged over wet days with daily precipitation not less than 1 mm. We use the area-weighted method to calculate the regional average. To keep consistency between the model simulations and observations, all of the datasets used in this study are remapped onto the same horizontal resolution and masked with HadGHCND. After that, the observed and

model-simulated extreme climate indices are calculated based on the definitions of the employed ETCCDI over each grid for each model.

We employ the skill score to quantify the performances of the CMIP5 models in simulating the spatial patterns of the climatological extreme temperature and precipitation indices in Central Asia (Taylor 2001; Hirota et al. 2011; Song and Zhou 2014). The definition of the skill score can be expressed as:

$$\text{Skill Score} = \frac{(1 + R)^2}{\left(\text{SDR} + \frac{1}{\text{SDR}}\right)} \quad (1)$$

**Table 3** Definitions of the extreme climate indices used in this study

Index	Name	Definitions	Unit
TNn	Coldest night	Annual minimum value of daily minimum temperature	°C
TNx	Warmest night	Annual maximum value of daily minimum temperature	°C
TXn	Coldest day	Annual minimum value of daily maximum temperature	°C
TXx	Warmest day	Annual maximum value of daily maximum temperature	°C
CDD	Dry days	Annual maximum length of dry days with daily precipitation less than 1 mm	days
RX1 day	1-day maximum precipitation	Annual maximum 1-day precipitation amount	mm
RX5 day	5-day maximum precipitation	Annual maximum consecutive 5-day precipitation amount	mm
SDII	Precipitation intensity	Simple precipitation intensity index averaged over days with daily precipitation not less than 1 mm	mm day <sup>-1</sup>

Here,  $R$  is the pattern correlation between the observations and model simulations. SDR is the standard deviation ratio between the model simulation and observation.

Note that part of the Tibetan Plateau (TP) is located in arid Central Asia (gray shading in Fig. 1). CMIP5 models show an obvious cold bias in simulating the observed temperature over the TP, which results from both the limitation in the model parameterization of physical processes and the uncertainty of the observations (because the observations are

interpolated from nearby stations with low elevations, but the temperature is highly dependent on elevation) (Su et al. 2013; Chen and Frauenfeld 2014; Chen et al. 2017; Palazzi et al. 2017). This cold bias can strongly affect future projections of the whole region. In addition, the TP is generally regarded in many studies as a specific high-altitude region that should be separately discussed (Su et al. 2013; Zhang et al. 2017; You et al. 2018). Thus, in this study, we focus on the region of Central Asia, with the TP masked out.

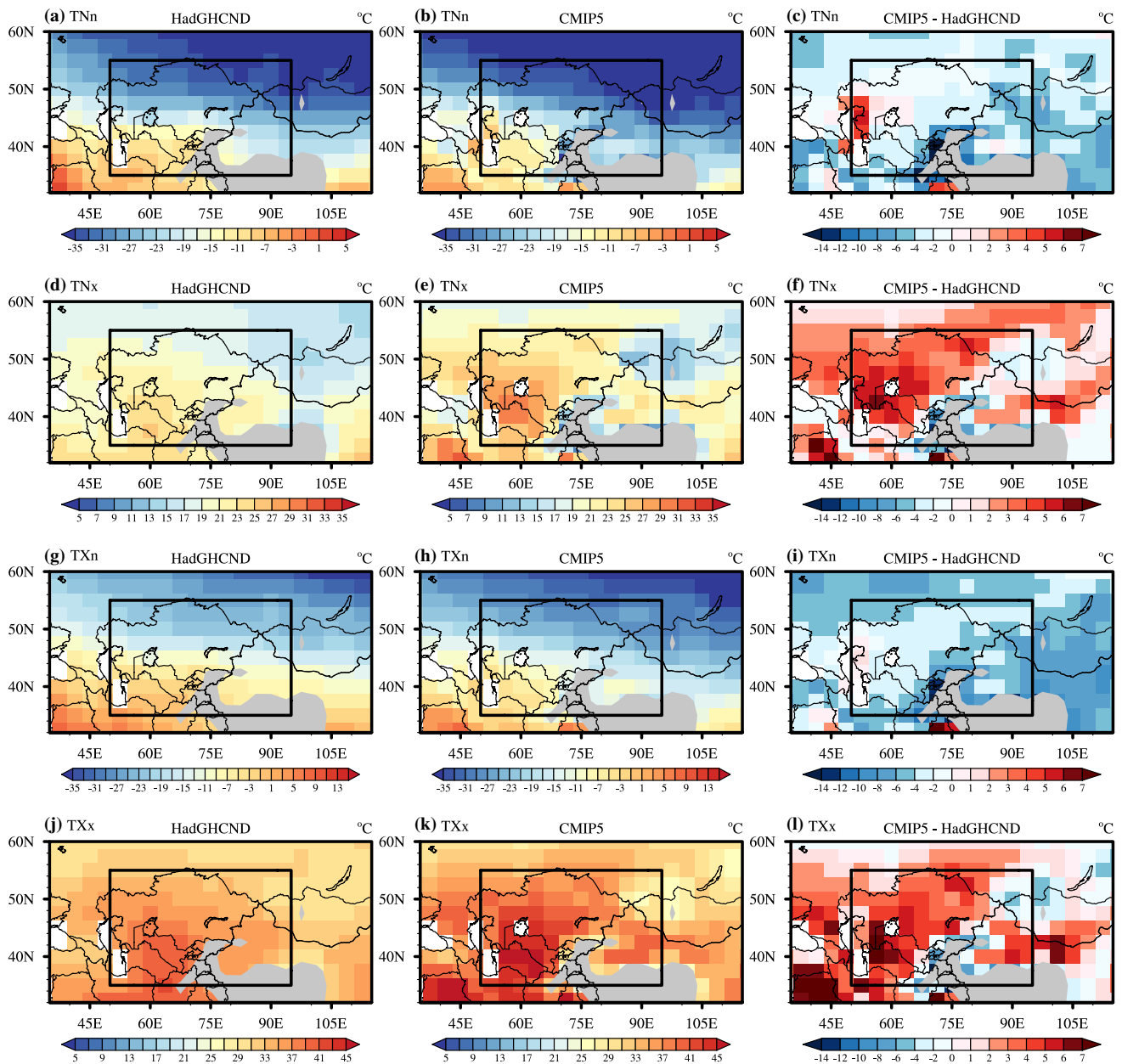


**Fig. 1** Spatial patterns for the climatological mean extreme temperature indices (unit: °C) during 1986–2005. The left, middle, and right columns indicate the results from the HadGHCND, CMIP5 MME, and bias between the CMIP5 MME and HadGHCND, respectively.

The rows, from top to bottom, indicate TNn, TNx, TXn, and TXx. The black boxes indicate Central Asia (35–55°N, 50–95°E). Gray shadings denote the TP with elevations greater than 2500 m

### 2.3 Bias correction method

To correct the bias of climate models in simulating the changes in regional temperature and precipitation, many bias correction methods have been proposed in previous studies (Weiland et al. 2010; Dosio and Paruolo 2011; Teutschbein and Seibert 2012; Wu and Huang 2016). As in previous studies (Chen et al. 2011; Teutschbein and Seibert 2012), we employ a variance scaling method in this study to correct the historical and projected temperature and precipitation indices over Central Asia from CMIP5 models. This method can guarantee that the climatological mean and standard deviation of the model simulations during the reference period are the same as those of the observations, and the model biases are time variant. There are two steps to correct the model simulations based on this method.

1. The climatological means of the temperature and precipitation indices are corrected based on the “delta change” method:

$$T_{ij}(d) = T_{sim,ij} + (\bar{T}_{obs,ij} - \bar{T}_{ref,ij}) \quad (2)$$

$$P_{ij}(d) = P_{sim,ij} \times \left( \frac{\bar{P}_{obs,ij}}{\bar{P}_{ref,ij}} \right) \quad (3)$$

Here,  $T_{ij}(d)$  and  $P_{ij}(d)$  indicate the bias-corrected temperature and precipitation indices for each grid (i, j), respectively.  $\bar{T}_{obs,ij}$  ( $\bar{P}_{obs,ij}$ ) and  $\bar{T}_{ref,ij}$  ( $\bar{P}_{ref,ij}$ ) are the climatological mean temperature (precipitation) indices from the observations and model simulations during the reference period (1986–2005), respectively. Note we assume that 20 years of observations are enough to represent the climate variability of the region for model evaluation.  $T_{sim,ij}$  and  $P_{sim,ij}$  are the model-simulated temperature and precipitation indices from both historical and future projection simulations, respectively. Note that all of the extreme indices are corrected based on the method for each model run.

2. The long-term mean (denoted as  $\bar{(\ )}$ ) of the delta change corrected historical ( $P_{ref,ij}(d)$ ) and the projected ( $P_{rcp,ij}(d)$ ) precipitation indices are removed to obtain the corresponding anomalies (denoted by  $(\prime)$ ):

$$P'_{ref,ij}(d) = P_{ref,ij}(d) - \bar{P}_{ref,ij}(d) \quad (4)$$

$$P'_{rcp,ij}(d) = P_{rcp,ij}(d) - \bar{P}_{rcp,ij}(d) \quad (5)$$

After that, the anomalies of the model simulations from Eqs. (4) and (5) are scaled by the ratio of the observed

( $\sigma(P_{obs,ij})$ ) and model-simulated standard deviations ( $\sigma(P_{ref,ij}(d))$ ):

$$P'^*_{ref,ij} = P'_{ref,ij}(d) \times \left[ \frac{\sigma(P_{obs,ij})}{\sigma(P_{ref,ij}(d))} \right] \quad (6)$$

$$P'^*_{rcp,ij}(d) = P'_{rcp,ij}(d) \times \left[ \frac{\sigma(P_{obs,ij})}{\sigma(P_{ref,ij}(d))} \right] \quad (7)$$

Finally, the corrected historical ( $P_{refcor,ij}(d)$ ) and future projection ( $P_{rcpcor,ij}(d)$ ) indices are achieved by adding the scaled anomalies back to the climatological mean values:

$$P_{refcor,ij}(d) = P'^*_{ref,ij}(d) + \bar{P}_{ref,ij}(d) \quad (8)$$

$$P_{rcpcor,ij}(d) = P'^*_{rcp,ij}(d) + \bar{P}_{rcp,ij}(d) \quad (9)$$

Note that the temperature indices are corrected based on the same method in step 2.

### 2.4 The timing of models in reaching 1.5 and 2 °C global warming

The 21-year time-slice approach is employed in this study to discern the impacts of 1.5 and 2 °C global warming. This approach can eliminate the uncertainties associated with climate sensitivities from the different models and allow us to consider the nonlinearities in extreme indices resulting from internal variability (Hawkins et al. 2014; Schleussner et al. 2016; James et al. 2017).

For each model, the timing of 1.5 and 2 °C global warming is defined as the first instance when the 21-year running mean of the global surface air temperature reaches 1.5 and 2 °C, respectively, above the preindustrial era level (1861–1890) (Table 1). The MME of the CMIP5 future projections in 1.5 and 2 °C warmer worlds (relative to the present period of 1986–2005) is the equal weighted average of the corresponding changes from different models averaged over a 21-year window centered over the warming threshold occurrence.

### 2.5 Avoided intensification of extreme indices between the 1.5 and 2 °C warming levels

As in previous studies (Li et al. 2018a), the avoided intensification of extreme indices can be expressed as:

$$\text{Avoided intensification} = \frac{C2.0 - C1.5}{C2.0} \times 100 \% \quad (10)$$

Here,  $C1.5$  and  $C2.0$  indicate the changes at the 1.5 and 2 °C global warming levels with respect to the reference

period (1986–2005), respectively. This reference period is widely used in previous studies (IPCC 2013; Schleussner et al. 2016). Note avoided intensification percentages would be larger with a more recent baseline.

## 2.6 Response of extreme events to global warming and the signal-to-noise ratio

There are two steps used to calculate the response of extreme events to global warming (Zhang et al. 2018): (1) the 5-year overlapping mean over decadal periods (i.e., 2006–2015, 2011–2020, up to 2086–2095) is employed on the projected extreme indices averaged over Central Asia and global mean near-surface air temperature to obtain the time series, and (2) the linear regression between them is derived as the response rate. Note that the response rate is calculated separately in each model.

The signal-to-noise ratio (SNR) is defined as the ratio of the multimodel ensemble median and the intermodel standard deviation (Pendergrass et al. 2015). The changes are robust if SNRs are greater than 1. The uncertainties of future projections are estimated based on ranking individual model simulations.

## 3 Results

### 3.1 Performance of the CMIP5 models in simulating extreme climate events

The observed and model-simulated spatial patterns of the climatological extreme temperature indices during 1986–2005 are shown in Fig. 1. The observed TNn, TNx, TXn, and TXx in Central Asia decrease from southwest to northeast (Fig. 1a, d, g, and j). The spatial distributions of these indices can be well captured by the CMIP5 MME (Fig. 1b, e, h, and k). With respect to the observations, the CMIP5 MME underestimates the cold indices (TNn and TXn) but overestimates the warm indices (TNx and TXx) over nearly all of Central Asia, with a strong cooling center (lower than  $-6\text{ }^{\circ}\text{C}$ ) in the southern region and a warming center (higher than  $3\text{ }^{\circ}\text{C}$ ) in the western region.

We further show the observed and model-simulated spatial patterns of the mean states of the four precipitation extreme indices in Central Asia in Fig. 2. The observed CDD decreases from the southern to the northern parts of Central Asia, with two centers in Turkmenistan (longer than 140 days) and the Taklimakan Desert (approximately 116 days) (Fig. 2a). The meridional distribution and the locations of these two centers of observed CDD are well captured by the CMIP5 MME (Fig. 2b). The observed CDD is overestimated by the CMIP5 MME over nearly the whole region (approximately 16%), except for the northwestern

and northeastern parts (Fig. 2c). The absolute magnitude of the underestimated CDD over the northeastern part (32%) is much larger than that over the northwestern part (4%) of Central Asia. This results from the stronger overestimation of dry days (daily precipitation less than 1 mm) over the northwestern part than over the other part of this region (figure not shown).

The observed RX1 day, RX5 day, and SDII show a zonal tri-pole distribution, with two dry centers over south Kazakhstan and Xinjiang in western China and one wet center over the mountain regions between those two locations (Fig. 2d, g, and j). The magnitudes of the observed RX1 day, RX5 day, and SDII over the dry (wet) centers are approximately 7 mm, 18 mm, and  $2.4\text{ mm day}^{-1}$  (25 mm, 50 mm, and  $5.2\text{ mm day}^{-1}$ ), respectively. The locations of the observed dry/wet centers for RX1 day, RX5 day, and SDII are well captured by the CMIP5 MME (Fig. 2e, h, and k). However, these indices are overestimated by the CMIP5 MME over nearly all of Central Asia, with the largest bias occurring in the southeastern part at a magnitude larger than 40% (Fig. 2f, i, and l). The overestimations of the precipitation indices (RX1 day, RX5 day, and SDII) are associated with the overestimated frequency of observed rain events, ranging from 1 to  $10\text{ mm day}^{-1}$ , i.e., the so-called “drizzling too much” phenomenon revealed by climate models in previous studies (Stephens et al. 2010).

In terms of the regional average, TNn, TXn, and CDD (TNx, TXx, RX1 day, RX5 day, and SDII) are underestimated (overestimated) by the CMIP5 MME, with absolute values of  $2.9\text{ }^{\circ}\text{C}$ ,  $4.3\text{ }^{\circ}\text{C}$ , and 8% ( $2.0\text{ }^{\circ}\text{C}$ ,  $2.5\text{ }^{\circ}\text{C}$ , 13%, 23%, and 10%), respectively (Figs. S1 and S2). The corresponding overestimations and underestimations are found in most of the models used in this study. The magnitudes of the model biases for the extreme indices show a large range, which can be partly associated with the model convective schemes. For instance, the models that overestimate observed TNn (CDD) mainly come from the “A” (“T”) scheme group (Figs. S1a and S2a).

The performances of the CMIP5 models in capturing the climatological mean extreme indices in Central Asia are quantified, as shown in Fig. 3. The pattern correlations of the cold indices (TXn and TNn) are higher than 0.7 for all of the models (Fig. 3a). The models tend to show a higher pattern correlation for cold indices (TXn and TNn) than the other extreme indices. All models underestimate the observed standard deviations of TXx and TNx (Fig. 3b). The models from the “A” scheme group tend to underestimate (overestimate) the observed standard deviations of the temperature (precipitation) indices. Considering the influence of both pattern correlation and ratio of the standard deviation to the observations, the CMIP5 models tend to show high skill scores for the cold indices (TNn and TXn), followed by the precipitation

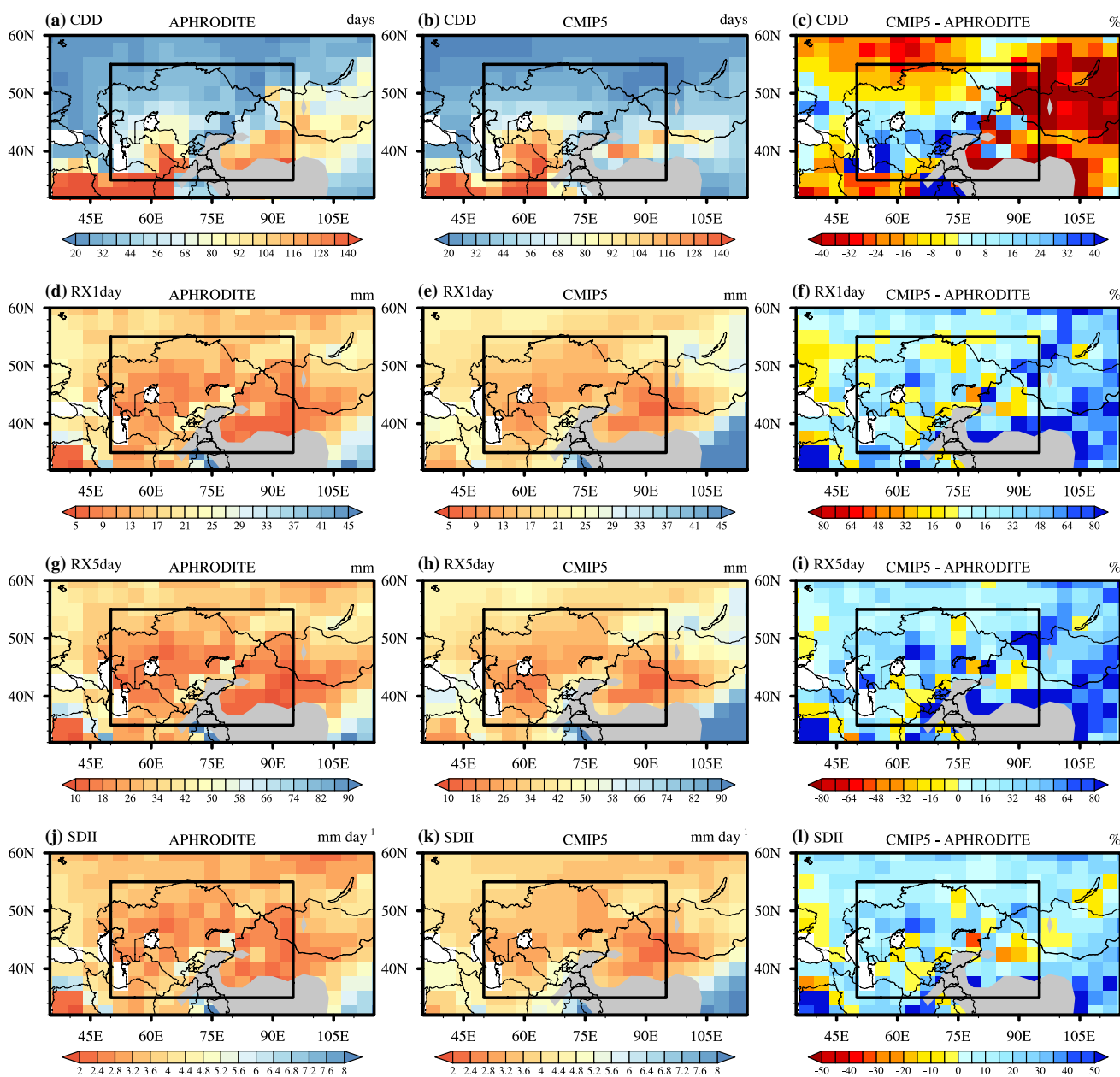


**Fig. 2** Spatial patterns of the climatological mean extreme precipitation indices during 1986–2005. The left, middle, and right columns indicate the results from APHRODITE, CMIP5 MME, and the bias between the CMIP5 MME and APHRODITE, respectively. The

rows, from top to bottom, indicate the CDD (days), RX1 day (mm), RX5 day (mm), and SDII ( $\text{mm day}^{-1}$ ), respectively. The unit for the model bias in the right column is %

indices (CDD, RX1 day, RX5 day, and SDII) and warm indices ( $\text{TX}_x$  and  $\text{TN}_x$ ) (Fig. 3c). The skill scores of the CMIP5 MME are higher than those of most models for all extreme indices in Central Asia. A large range of model skill scores can be found for the warm temperature and precipitation indices. The CMIP5 models show high performance in simulating the climatological spatial patterns of the observed surface air temperature. The skill scores of the CMIP5 models in simulating the spatial patterns

of the climatological mean extreme indices over Central Asia are not sensitive to the convective schemes (Fig. 3c).

The above results reveal that the CMIP5 MME can generally reproduce the observed spatial patterns of historical extreme events in Central Asia. However, obvious biases are also found in some models in simulating the extreme indices, resulting in a large range of corresponding skill scores. Thus, we employ a bias correction method (see Sect. 2.3) to constrain future projections



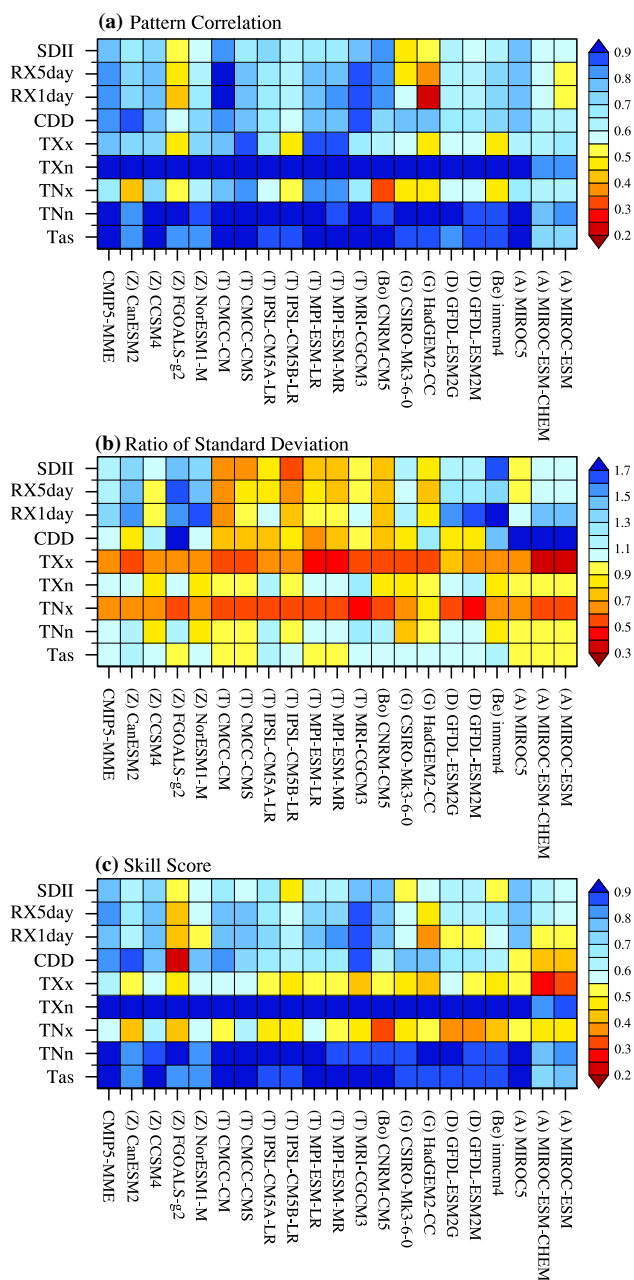


**Fig. 3** The skills of the CMIP5 models in simulating the spatial patterns of the mean state of extreme climate indices in Central Asia during 1986–2005. **a** Pattern correlation; **b** ratio of the model-simulated standard deviation to the observations; **c** skill score. “A”, “Be”, “Bo”, “D”, “G”, “T”, and “Z” in the parentheses denote the model-employed convective schemes utilized, as listed in Table 2

based on the observations before addressing the future changes in extreme events over Central Asia. In the following section, the results are derived from the bias-corrected future projections.

### 3.2 Response of extreme events to global warming

The projected changes in the regionally averaged extreme indices in Central Asia under the RCP4.5 (blue lines) and RCP8.5 (red lines) scenarios are shown in Fig. 4. All of the extreme temperature indices would increase robustly (based on the signal-to-noise ratio test) during the twenty-first century, at rates of 0.37 (25–75% uncertainties: 0.28–0.44) and 0.80 (0.65–1.03) °C decade<sup>-1</sup> for TNn, 0.20 (0.15–0.25) and 0.50 (0.43–0.61) °C decade<sup>-1</sup> for TNx, 0.34 (0.27–0.41) and 0.68 (0.58–0.84) °C decade<sup>-1</sup> for TXn, and 0.22 (0.18–0.28) and 0.53 (0.44–0.60) °C decade<sup>-1</sup> for TXx under the RCP4.5 and RCP8.5 scenarios, respectively (Table 4). The higher the RCPs are, the larger the increasing rates. The increasing rates of the cold indices (TNn and TXn) are larger than those of the warm indices (TNx and TXx). At the end of the twenty-first century, TNn, TNx, TXn, and TXx under the RCP8.5 scenario would increase by 7.52 (6.11–9.68) °C, 4.70 (4.04–5.73) °C, 6.39 (5.45–7.90) °C, and 4.98 (4.14–5.64) °C, respectively.

During the twenty-first century, RX1 day, RX5 day, and SDII would also increase robustly at rates of 1.22 (0.90–1.63) % decade<sup>-1</sup>, 1.16 (0.83–1.52) % decade<sup>-1</sup>, and 0.87 (0.60–1.11) % decade<sup>-1</sup> under the RCP4.5 scenario and rates of 2.84 (2.13–3.66) % decade<sup>-1</sup>, 2.43 (2.03–3.21) % decade<sup>-1</sup>, and 2.00 (1.43–2.69) % decade<sup>-1</sup> under the RCP8.5 scenario, respectively (Table 4). At the end of the twenty-first century, RX1 day, RX5 day, and SDII under the RCP8.5 scenario would increase by 26.70% (20.02–34.40%), 22.84% (19.08–30.17%), and 18.80% (13.44–25.29%), respectively. In contrast, the CDD would increase under both the RCP4.5 and RCP8.5 scenarios at rates of 0.07 (– 0.15 to 0.56) % decade<sup>-1</sup> and 0.34 (– 0.46 to 1.30) % decade<sup>-1</sup>, respectively, showing large intermodel uncertainty (Fig. 4e).

We further show the responses of projected extreme climate events changes in Central Asia to global mean near-surface air temperature (Figs. 5 and 6). Both the temperature and precipitation extreme indices respond approximately linearly to global warming (Fig. 5). Except for the CDD, these responses are robust against the model spread, with high signal-to-noise ratios (Fig. 6). The response rates of the cold indices are larger than those of the warm indices, with rates of 1.93 (1.62–2.14) °C K<sup>-1</sup> for TNn and 1.71 (1.44–1.85) °C K<sup>-1</sup> for TXn compared to rates of 1.18 (1.00–1.23) °C K<sup>-1</sup> for TNx and 1.25 (1.12–1.40) °C K<sup>-1</sup> for TXx under the RCP8.5 scenario. The larger response rates of the cold indices compared to those of the warm indices result from a faster increasing rate of winter temperature than summer temperature (Peng et al. 2019). The response rates of the extreme wet indices are higher than those of precipitation intensity, with rates of 6.30 (5.62–7.68) % K<sup>-1</sup>, 5.71 (4.93–6.61) %

**Fig. 4** The 21-year running mean of the anomalies of the regionally averaged corrected extreme climate indices over Central Asia during 1979–2099 (relative to the period 1986–2005). **a** TNn; **b** TNx; **c** TXn; **d** TXx; **e** CDD; **f** RX1 day; **g** RX5 day; **h** SDII. The blue and red lines indicate the projections from the CMIP5 MME under the RCP4.5 and RCP8.5 scenarios, respectively. Shadings indicate the 25–75% uncertainties. The black and gray colors indicate the corresponding results from the historical simulations. The units for the extreme temperature and precipitation indices are °C and %, respectively

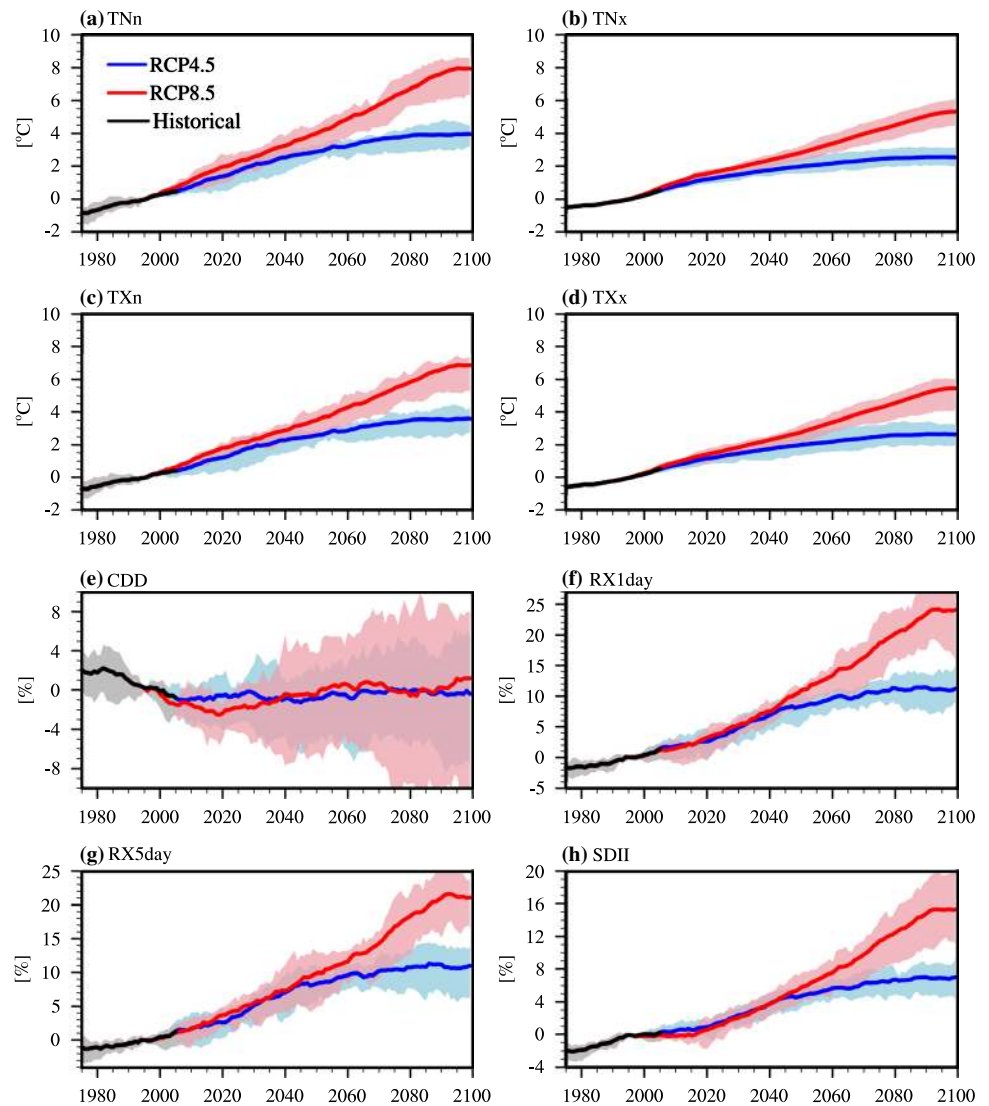


**Table 4** Projected trends and the 25–75% uncertainties of the extreme climate indices over Central Asia during 2006–2099 from the CMIP5 projections

Extreme Index	RCP4.5	RCP8.5	Unit	SNR (RCP4.5/8.5)
TNn	<b>0.37</b> (0.28–0.44)	<b>0.80</b> (0.65–1.03)	°C decade <sup>-1</sup>	<b>2.80/4.10</b>
TNx	<b>0.20</b> (0.15–0.25)	<b>0.50</b> (0.43–0.61)	°C decade <sup>-1</sup>	<b>3.23/3.97</b>
TXn	<b>0.34</b> (0.27–0.41)	<b>0.68</b> (0.58–0.84)	°C decade <sup>-1</sup>	<b>2.50/3.72</b>
TXx	<b>0.22</b> (0.18–0.28)	<b>0.53</b> (0.44–0.60)	°C decade <sup>-1</sup>	<b>2.70/3.64</b>
CDD	0.07 (– 0.15 to 0.56)	0.34 (– 0.46 to 1.30)	% decade <sup>-1</sup>	0.35/0.20
RX1 day	<b>1.22</b> (0.90–1.63)	<b>2.84</b> (2.13–3.66)	% decade <sup>-1</sup>	<b>2.25/3.07</b>
RX5 day	<b>1.16</b> (0.83–1.52)	<b>2.43</b> (2.03–3.21)	% decade <sup>-1</sup>	<b>2.18/2.82</b>
SDII	<b>0.87</b> (0.60–1.11)	<b>2.00</b> (1.43–2.69)	% decade <sup>-1</sup>	<b>2.20/3.13</b>

The bold fonts indicate that the trends have high signal-to-noise ratios (greater than 1)

$K^{-1}$ , and 4.99 (3.63–5.33) %  $K^{-1}$  for RX1 day, RX5 day, and SDII, respectively, under the RCP8.5 scenario. The response rates under the RCP4.5 scenario change slightly with respect to those under the RCP8.5 scenario (Figs. 6 and S3).

### 3.3 Changes in extreme events in Central Asia under 1.5 and 2 °C global warming

The spatial patterns of the changes in extreme temperature and precipitation events at the 1.5 and 2 °C global warming

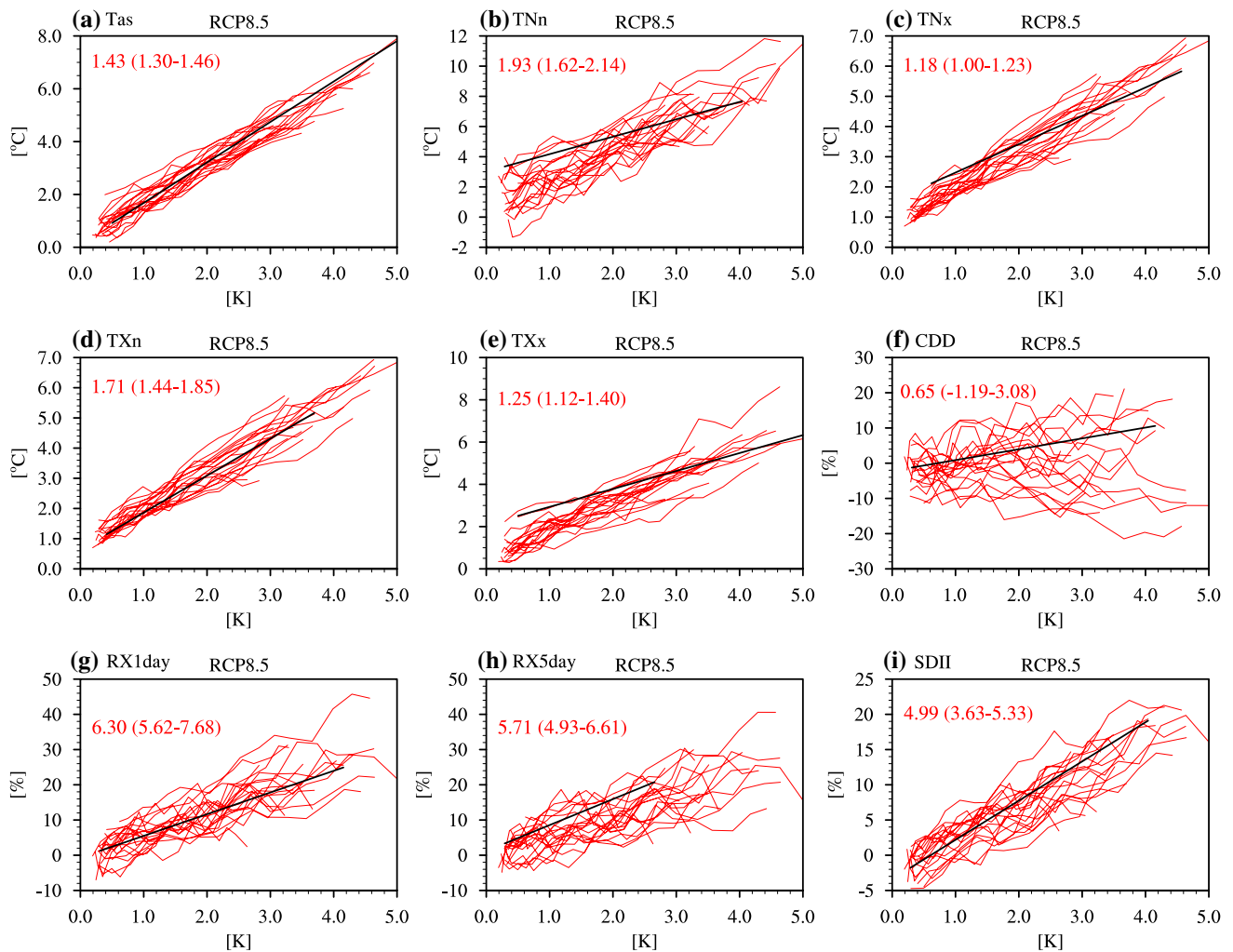


**Fig. 5** Responses of corrected extreme events averaged over Central Asia (vertical coordinates) to global near-surface air temperature changes (horizontal coordinates) under the RCP8.5 scenario. **a** Surface air temperature (Tas); **b** TNn; **c** TNx; **d** TXn; **e** TXx; **f** CDD; **g** RX1 day; **h** RX5 day; **i** SDII. Projected changes are calculated over decadal periods starting in 2006, with an overlap of 5 years (i.e.,

2006–2015, 2011–2020, up to 2081–2095). Each red line represents an individual model, and the black line denotes the linear fit of the median response. The red strings in the top left figure indicate the multimodel median scaling rates and the 25–75% uncertainties for the temperature ( $^{\circ}\text{C K}^{-1}$ ) and precipitation ( $\% \text{K}^{-1}$ ) indices

levels (relative to 1986–2005) under the RCP8.5 scenario are shown in Figs. 7 and 8, respectively. Compared with the present period (1986–2005), in a  $1.5^{\circ}\text{C}$  warmer world, both the cold (Fig. 7a, g) and warm (Fig. 7d, j) indices would consistently increase (more than 70% of the models with the same sign of change) over Central Asia but show different spatial patterns, which may be partly due to the influence of internal variability. The warming magnitudes for the cold indices increase from the southeastern to northwestern parts of the region, with a strong warming center in northern Kazakhstan (larger than  $2.6^{\circ}\text{C}$ ). This is associated with the distribution of corresponding changes in the winter mean surface air temperature, which shows a larger increasing rate at higher latitudes (figure not shown). In contrast, the warm

indices increase evenly across Central Asia at a value of approximately  $1.5^{\circ}\text{C}$ .

Meanwhile, both extreme wet indices (RX1 day and RX5 day) and the mean precipitation intensity (SDII) would increase over nearly all of Central Asia but with low consistency (less than 70% of the models have the same sign of change) over most regions (Fig. 8d, g and j). Three centers are found for RX5 day over the southeastern, central southern and northern regions, with a value greater than 5%, while a center over the northeastern region for the SDII is projected at a rate of approximately 3%. The CDD would increase over the western region (2%) but decrease over the eastern and northern regions ( $-2\%$ ) with low consistency (Fig. 8a).

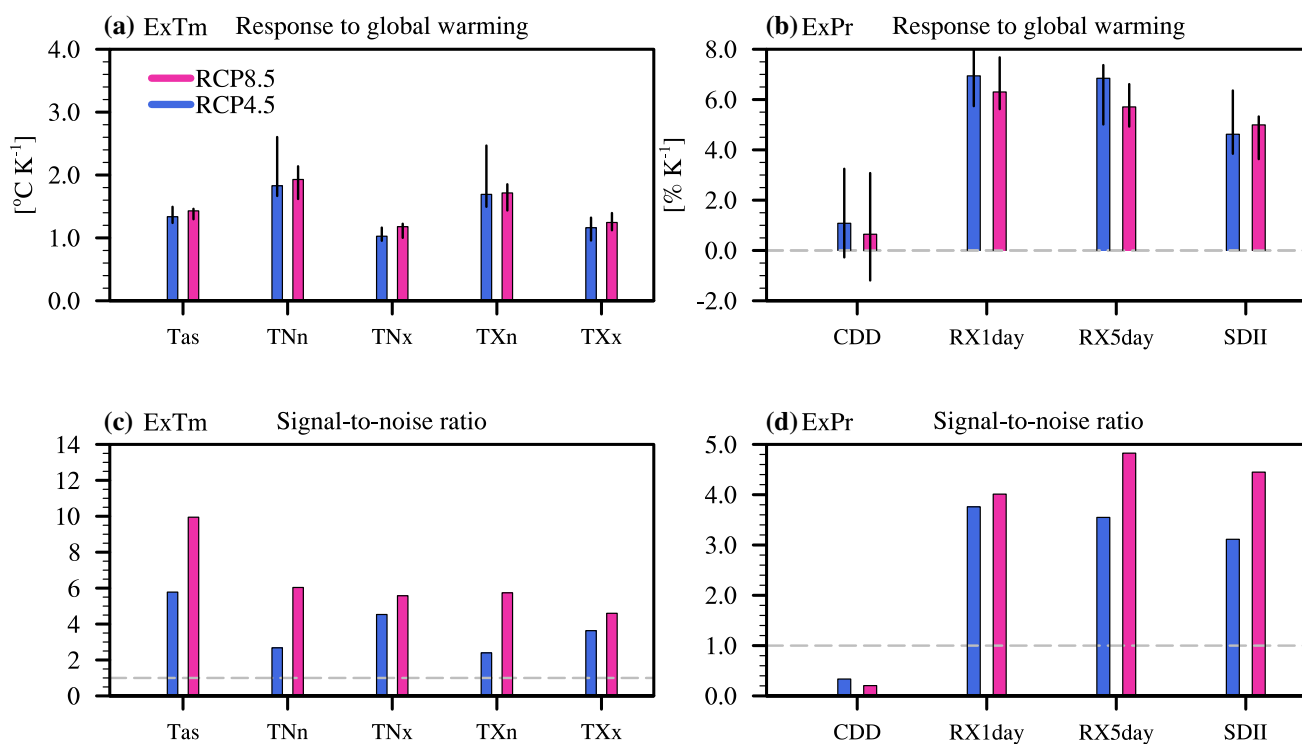


**Fig. 6** Response rates of the corrected extreme indices over Central Asia to the changes in global mean surface air temperature under the RCP4.5 (blue bars) and RCP8.5 (red bars) scenarios. **a** Temperature extreme indices ( $^{\circ}\text{C K}^{-1}$ ). **b** Precipitation extreme indices ( $\% \text{K}^{-1}$ ).

The multimodel ensemble medians and the 25–75% uncertainties are denoted by histograms and vertical black lines, respectively. **c**, **d** show the signal-to-noise ratios of the temperature and precipitation extremes, respectively

In a  $2^{\circ}\text{C}$  warmer world, the spatial patterns of the changes in both the extreme temperature and precipitation indices across Central Asia are similar to those in a  $1.5^{\circ}\text{C}$  warmer world. The cold indices would increase by more than  $1.8^{\circ}\text{C}$  over nearly the whole region, with a warming center in the northwestern part higher than  $3.6^{\circ}\text{C}$ , while the warm indices would evenly increase by approximately  $1.8^{\circ}\text{C}$ . RX1 day, RX5 day, and SDII would increase consistently over nearly all of Central Asia by more than 7%, 5%, and 4%, respectively.

Compared with the results in a  $1.5^{\circ}\text{C}$  warmer world,  $0.5^{\circ}\text{C}$  more warming would consistently increase TNn and TXn over nearly the whole region, with the warming centers in the northern part of the region with values larger than  $1.2^{\circ}\text{C}$  and  $0.8^{\circ}\text{C}$ , respectively. Meanwhile, TNx and TXx would consistently increase over Central Asia, with values larger than  $0.4^{\circ}\text{C}$ . RX1 day, RX5 day, and SDII would increase over nearly all of Central Asia in response to  $0.5^{\circ}\text{C}$  more warming, with high consistency for RX5 day and SDII in the northwestern and northern regions. The CDD would increase over most regions of Central Asia, with low model consistency.

The spatial distributions of projected changes in the extreme temperature and precipitation indices under the RCP4.5 scenario are generally similar to those under the

RCP8.5 scenario (Figs. S4 and S5). However, there are still some differences between these two scenarios. The increasing magnitudes of TNn, TNx, TXn, and TXx would be lower in a  $1.5^{\circ}\text{C}$  warmer world under RCP4.5 over the whole region. The areas with consistent signs of changes for CDD, RX1 day, RX5 day, and SDII are larger in a  $1.5^{\circ}\text{C}$  warmer world under the RCP4.5 scenario. In response to  $0.5^{\circ}\text{C}$  more warming, the increases in TNn, TXn, and RX5 day (TNx, TXx, CDD, and SDII) would be larger (lower) under the RCP4.5 scenario over nearly all of Central Asia.

We further quantified the avoided intensification of extreme indices in Central Asia from  $0.5^{\circ}\text{C}$  less warming, as shown in Fig. 9. If global warming can be limited to  $1.5^{\circ}\text{C}$  instead of  $2^{\circ}\text{C}$ , Central Asia is projected to benefit from a consistently (the same sign of changes in more than 70% of the models) avoided intensification for both extreme temperature (TNn, TNx, TXn, and TXx) and precipitation (RX1 day, RX5 day, and SDII) events. Under the RCP8.5 scenario, TNx and TXx would increase by  $1.82$  ( $1.60$ – $2.17$ )  $^{\circ}\text{C}$  and  $1.79$  ( $1.31$ – $2.14$ )  $^{\circ}\text{C}$  with respect to the present day for the  $1.5^{\circ}\text{C}$  warming level, respectively, compared with  $2.25$  ( $2.12$ – $2.79$ )  $^{\circ}\text{C}$  and  $2.31$  ( $1.92$ – $2.91$ )  $^{\circ}\text{C}$  for the  $2^{\circ}\text{C}$  warming level, respectively (red bars in Fig. 9). Thus, the avoided intensification is estimated to be 24% (20–31%) and 29% (19–37%) for TNx and TXx due to  $0.5^{\circ}\text{C}$

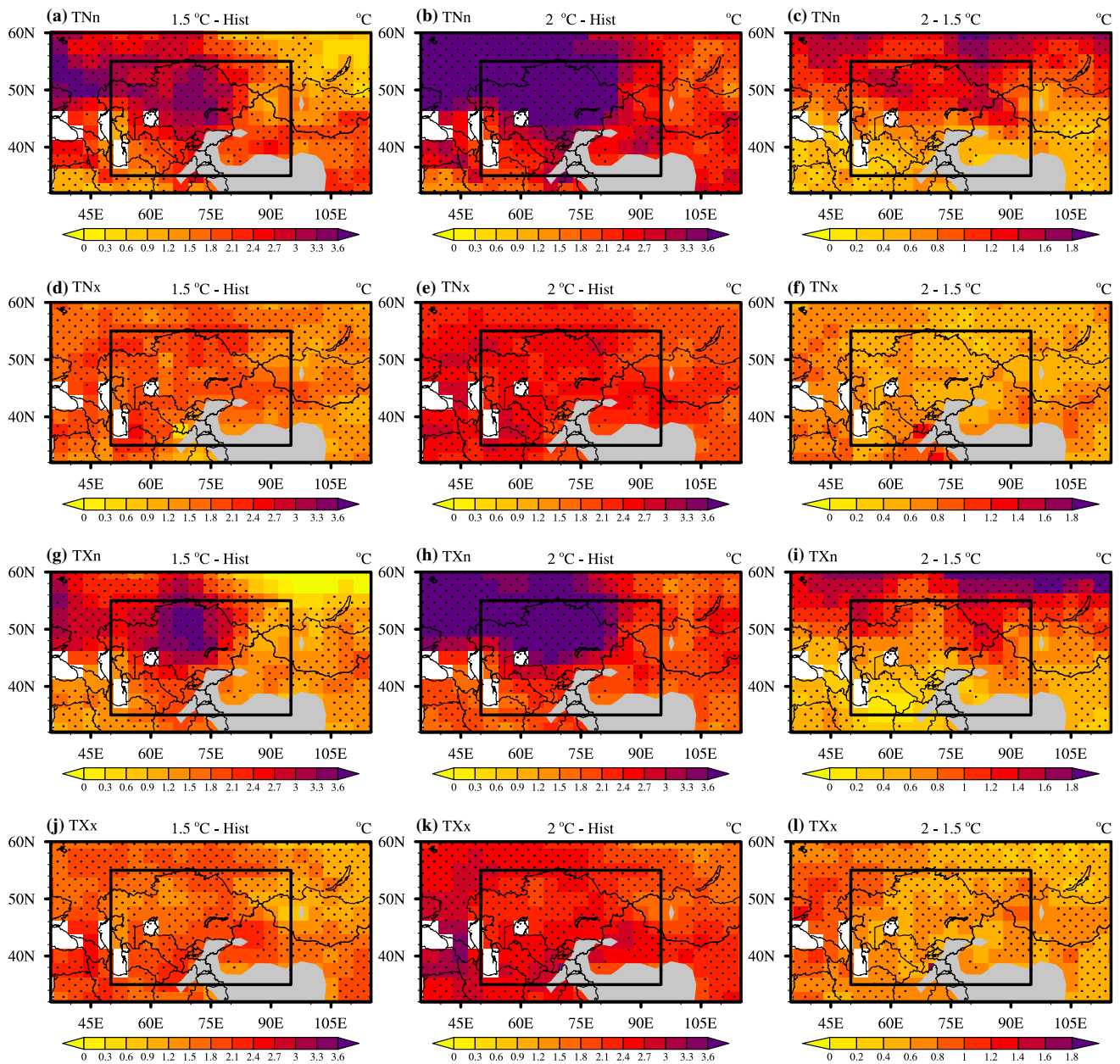


**Fig. 7** Spatial patterns for the changes in corrected extreme temperature indices (unit: °C) in 1.5 and 2 °C warmer worlds from the CMIP5 MME under the RCP8.5 scenario (relative to the period 1986–2005). The left, middle, and right columns show the results in

the 1.5 and 2 °C warmer worlds and the results due to an increase of 0.5 °C, respectively. The rows, from top to bottom, denote TNn, TNx, TXn, and TXx. Dots indicate where more than 70% of the models agree on the sign of the changes (the same applies below)

less warming, respectively. This robust reduction can also be seen for TNn [33% (18–55%)] and TXn [32% (10–51%)] under RCP8.5. The reduced risk under 0.5 °C less warming can also be seen for RX1 day [39% (26–61%)], RX5 day [42% (14–63%)], and SDII [53% (31–70%)].

Compared with the results under the RCP8.5 scenario, the avoided intensification of TNn, TNx, TXn, and TXx (RX1 day and SDII) tended to be larger (smaller) under the RCP4.5 scenario, suggesting a degree of scenario dependence. The

estimated avoided intensification for the CDD shows large uncertainty under both the RCP4.5 and RCP8.5 scenarios.

### 4 Summary and discussion

The 2015 Paris agreement committed to hold the increase in global mean temperature to well below 2 °C and to pursue efforts to limit the global mean temperature to 1.5 °C above

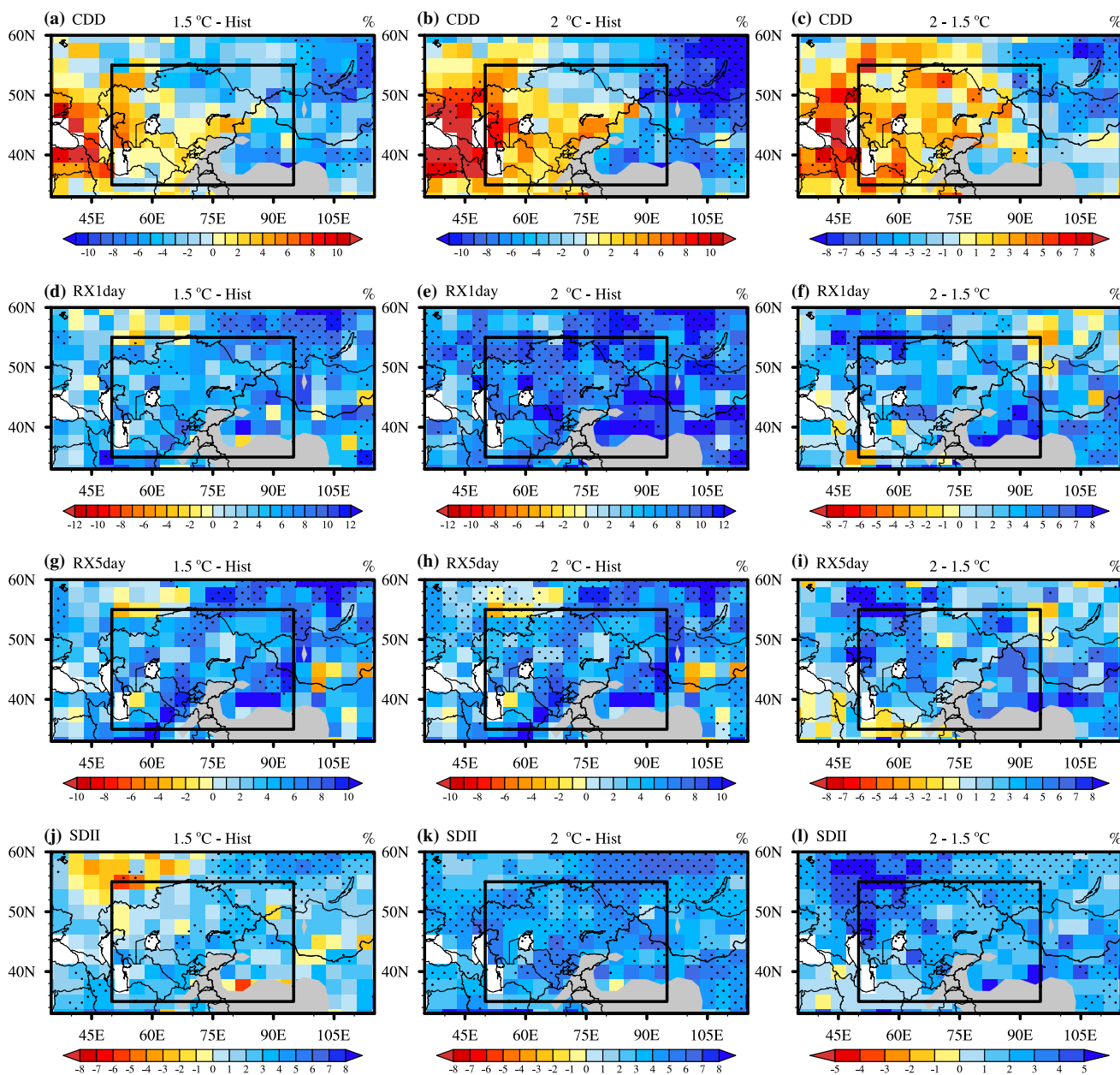


**Fig. 8** Spatial patterns for the changes in corrected extreme precipitation indices (unit: %) in 1.5 and 2 °C warmer worlds from the CMIP5 MME under the RCP8.5 scenario. The left, middle, and right col-

umns show the results in 1.5 and 2 °C warmer worlds and the results due to an increase of 0.5 °C, respectively. The rows, from top to bottom, denote CDD, RX1 day, RX5 day, and SDII

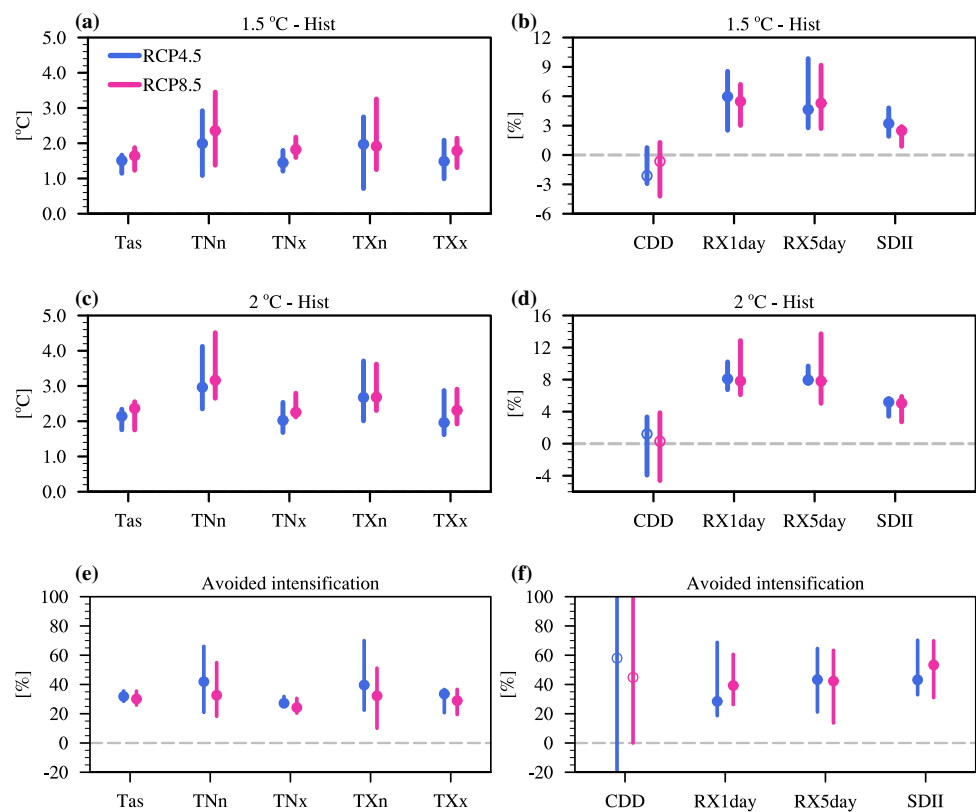
preindustrial levels, aiming to avoid the dangerous risk of climate change as a result of anthropogenic influence. Arid Central Asia is highly sensitive to extreme climate changes. We employ eight extreme indices (TN<sub>n</sub>, TX<sub>n</sub>, TN<sub>x</sub>, TX<sub>x</sub>, CDD, RX1 day, RX5 day, and SDII) to evaluate the impacts of 1.5 °C and 2 °C global warming scenarios on the changes in extreme events over this arid region based on CMIP5 models. The main conclusions are summarized as follows:

The CMIP5 models tend to show reasonable performance in reproducing the spatial patterns for the mean states of all

selected extreme indices. The models tend to underestimate TN<sub>n</sub>, TX<sub>n</sub>, and CDD but overestimate TN<sub>x</sub>, TX<sub>x</sub>, RX1 day, RX5 day, and SDII. A large range of model biases is found for all employed extreme indices. Therefore, a bias correction method is employed to constrain the future projections based on the observations.

As revealed in the corrected projections, all of the selected extreme indices, except for the CDD, in Central Asia would increase robustly during the twenty-first century, with higher rates under higher RCPs. Under RCP4.5

**Fig. 9** The changes in corrected extreme indices averaged over Central Asia in 1.5 and 2 °C warmer worlds under the RCP4.5 (blue bars) and RCP8.5 (red bars) scenarios. The left and right columns show the results for the extreme temperature (°C) and precipitation (%) indices. The top and middle rows indicate the results for 1.5 and 2 °C global warming, respectively. The bottom row indicates the avoided intensification from 0.5 °C less warming. The circles and bars indicate the multimodel medians and the 25–75% uncertainties, respectively. Solid (open) circles indicate that more (less) than 70% of the models agree on the sign of the changes



(RCP8.5), the cold indices TNn and TXn would increase at rates of 0.37 (0.28–0.44) [0.80 (0.65–1.03)] °C decade<sup>-1</sup> and 0.34 (0.27–0.41) [0.68 (0.58–0.84)] °C decade<sup>-1</sup>, respectively, compared with the lower rates of the warm indices TNx and TXx [0.20 (0.15–0.25) (0.50 (0.43–0.61)] °C decade<sup>-1</sup> and 0.22 (0.18–0.28) [0.53 (0.44–0.60)] °C decade<sup>-1</sup>, respectively). The increasing rates are 1.22% (0.90–1.63%) [2.84% (2.13–3.66%)] decade<sup>-1</sup> for RX1 day and 1.16% (0.83–1.52%) [2.43% (2.03–3.21%)] decade<sup>-1</sup> for RX5 day, which are larger than those for the SDII, with a value of 0.87% (0.60–1.11%) [2.00% (1.43–2.69%)] decade<sup>-1</sup>, under RCP4.5 (RCP8.5). In response to 0.5 °C more warming under RCP8.5, the CDD would increase over most regions but decrease over the northeastern part, with low consistency. RX1 day, RX5 day, and SDII would increase over all of Central Asia but with high consistency over the southeastern, northwestern, and northern regions. The strong centers for TNn and TXn are found in the northwestern region; those for RX1 day, RX5 day, and SDII are found in the southeastern, northwestern, and northwestern regions, respectively, while no obvious strong centers are found for TNx and TXx.

The extreme indices, except for CDD, in Central Asia have approximately linear responses to global warming, with high signal-to-noise ratios under RCP8.5, with rates of 1.93 (1.62–2.14) °C K<sup>-1</sup> for TNn, 1.71 (1.44–1.85) °C K<sup>-1</sup> for TXn, 1.18 (1.00–1.23) °C K<sup>-1</sup> for TNx, 1.25

(1.12–1.40) °C K<sup>-1</sup> for TXx, 6.30% (5.62–7.68%) K<sup>-1</sup> for RX1 day, 5.71% (4.93–6.61%) K<sup>-1</sup> for RX5 day, and 4.99% (3.63–5.33%) K<sup>-1</sup> for SDII. The rates under RCP4.5 change slightly compared with those under RCP8.5.

The intensification of extreme events over Central Asia is reduced at the 1.5 °C global warming level compared with that at the 2 °C level, showing obvious scenario dependence. In response to 0.5 °C less warming under RCP8.5, robust reductions are found for TNn, TNx, TXn, TXx, RX1 day, RX5 day, and SDII, with reduced magnitudes of 33% (18–55%), 24% (20–31%), 32% (10–51%), 29% (19–37%), 39% (26–61%), 42% (14–63%), and 53% (31–70%), respectively. The avoided intensification is larger (smaller) under RCP4.5 for TNn, TNx, TXn, and TXx (RX1 day and SDII). Large uncertainties are found for the avoided intensification of CDD.

Finally, we highlight the need for observationally constrained projections. An obvious difference is observed in the projected changes of extreme indices over Central Asia between the bias-corrected and uncorrected results. The response rates of TNn, TNx, TXn, TXx and CDD (RX1 day, RX5 day, and SDII) to global warming derived from the corrected projections in Fig. 5 are smaller (larger) than the uncorrected projections in Fig. S6. Compared to the uncorrected results (Fig. S7), stronger warming centers exist in the north-central region of Central Asia in a 1.5 °C warmer world for the corrected TNn and TXn under

RCP8.5, resulting in weaker warming over this region in response to 0.5 °C more warming (Fig. 7). The increasing magnitudes of RX1 day, RX5 day, and SDII derived from the corrected projections (Fig. 8) are larger than those derive from the uncorrected results (Fig. S8) over nearly all of Central Asia in response to 0.5 °C more warming. The avoided intensification of uncorrected (corrected) SDII in Fig. S9 (Fig. 9) is larger (smaller) under RCP4.5 compared with that under RCP8.5.

The bias correction method used in this study mainly accounts for the bias in the climatological mean values. Obvious biases have been found for the CMIP5 models in simulating the historical trends of extreme indices (Fig. S10). The models tend to reproduce significant increasing trends in the observed warm (TN<sub>x</sub> and TX<sub>x</sub>) and cold (TN<sub>n</sub> and TX<sub>n</sub>) indices but with overestimated and underestimated magnitudes, respectively. Those overestimations (underestimations) can be explained by the overestimated (underestimated) summer (winter) warming trend in Peng et al. (2019). The models tend to capture the observed changes in CDD and RX5 day but fail to reproduce the slight decreases in RX1 day and SDII. Changes in regional precipitation are strongly influenced by internal climate variability, which cannot be well reproduced in the climate models (Stott et al. 2010; Hegerl and Zwiers 2011; Sarojini et al. 2016). Previous studies have suggested that the influence of internal variability on regional temperature and precipitation changes would be small in mid- and long-term climate projections (Hawkins and Sutton 2009, 2011), providing some reliance on the future projections in this study. However, the overestimations/underestimations of historical extreme events over Central Asia could result in potential biases in corresponding future projections.

The responses of extreme temperature and precipitation indices over Central Asia to global warming are nearly linear for the multi-model ensemble averages (Seneviratne et al. 2016). In comparison, the responses from individual model simulations look less linear, as seen in Fig. 5 of the revised manuscript. The linearities of extreme climate event changes over Central Asia response to global warming also vary in climate indices, with more linear for the responses of temperature indices than those of precipitation indices. Besides, King (2019) highlights that accelerated warming as a function of global warming will occur over Central Asia in summer under RCPs. However, the obvious non-linearities of temperature changes associated with global warming in summer cannot be found for the annual mean temperature in this study, implying the seasonal dependence of response linearity. Thus, the linearities of extreme climate events changes over Central Asia in response to global warming under RCPs would be addressed in details for further studies.

**Acknowledgements** This work is jointly supported by the Strategic Priority Research Program of the Chinese Academy of Sciences (Grant No. XDA20060102) and the International Partnership Program of Chinese Academy of Sciences (Grant No. 134111KY5B20160031). Dongdong Peng is supported by the National Natural Science Foundation of China (Grant No. 41575043). Lixia Zhang is supported by the Ministry of Science and Technology of China under Grant 2018YFA0606501. We also acknowledge the support from the Jiangsu Collaborative Innovation Center for Climate Change.

**Open Access** This article is distributed under the terms of the Creative Commons Attribution 4.0 International License (<http://creativecommons.org/licenses/by/4.0/>), which permits unrestricted use, distribution, and reproduction in any medium, provided you give appropriate credit to the original author(s) and the source, provide a link to the Creative Commons license, and indicate if changes were made.

## References

- Arakawa A, Schubert WH (1974) Interaction of a cumulus cloud ensemble with the large-scale environment, Part I. *J Atmos Sci* 31(3):674–701
- Avila FB, Dong S, Menang KP et al (2015) Systematic investigation of gridding-related scaling effects on annual statistics of daily temperature and precipitation maxima: a case study for south-east Australia. *Weather Clim Extrem* 9:6–16
- Betts AK (1986) A new convective adjustment scheme. Part I: observational and theoretical basis. *Q J R Meteorol Soc* 112(473):677–691
- Bougeault P (1985) A simple parameterization of the large-scale effects of cumulus convection. *Mon Weather Rev* 113(12):2108–2121
- Caesar J, Alexander L, Vose R (2006) Large-scale changes in observed daily maximum and minimum temperatures: creation and analysis of a new gridded data set. *J Geophys Res Atmos* 111:D05101
- Chen L, Frauenfeld OW (2014) Surface air temperature changes over the twentieth and twenty-first centuries in China simulated by 20 CMIP5 models. *J Clim* 27(11):3920–3937. <https://doi.org/10.1175/JCLI-D-13-00465.1>
- Chen J, Brissette FP, Leconte R (2011) Uncertainty of downscaling method in quantifying the impact of climate change on hydrology. *J Hydrol* 401(3–4):190–202
- Chen X, Liu Y, Wu G (2017) Understanding the surface temperature cold bias in CMIP5 AGCMs over the Tibetan Plateau. *Adv Atmos Sci* 34(12):1447–1460. <https://doi.org/10.1007/s00376-017-6326-9>
- Christensen JH, Krishna Kumar K, Aldrian E, An S, Cavalcanti I, Castro M, Dong W, Goswami P, Hall A, Kanyanga J, Kitoh A, Kossin J, Lau N, Renwick J, Stephenson D, Xie S, Zhou T (2013) Climate Phenomena and their Relevance for Future Regional Climate Change. In: *Climate Change 2013: the Physical Science Basis*. In: Contribution of Working Group I to the Fifth Assessment Report of the Intergovernmental Panel on Climate Change. Cambridge University Press, Cambridge, United Kingdom and New York, NY, USA
- Deng H, Chen Y, Shi X et al (2014) Dynamics of temperature and precipitation extremes and their spatial variation in the arid region of northwest China. *Atmos Res* 138:346–355. <https://doi.org/10.1016/j.atmosres.2013.12.001>
- Donat MG, Alexander LV, Yang H et al (2013) Global land-based datasets for monitoring climatic extremes. *Bull Am Meteor Soc* 94(7):997–1006



- Donner LJ (1993) A cumulus parameterization including mass fluxes, vertical momentum dynamics, and mesoscale effects. *J Atmos Sci* 50(6):889–906
- Dosio A, Fischer EM (2017) Will half a degree make a difference? Robust projections of indices of mean and extreme climate in Europe Under 1.5°C, 2°C, and 3°C global warming. *Geophys Res Lett* 45(2):935–944. <https://doi.org/10.1002/2017GL076222>
- Dosio A, Paruolo P (2011) Bias correction of the ENSEMBLES high-resolution climate change projections for use by impact models: Evaluation on the present climate. *J Geophys Res Atmos* 116(D16)
- Dunn R, Donat MG, Alexander LV (2014) Investigating uncertainties in global gridded datasets of climate extremes. *Clim Past* 10(6):2171–2199
- Emanuel KA (1991) A scheme for representing cumulus convection in large-scale models. *J Atmos Sci* 48(21):2313–2329
- Emanuel KA (1993) A cumulus representation based on the episodic mixing model: the importance of mixing and microphysics in predicting humidity. In: *The representation of cumulus convection in numerical models* (pp. 185–192). American Meteorological Society, Boston
- Gregory D, Rowntree PR (1990) A mass flux convection scheme with representation of cloud ensemble characteristics and stability-dependent closure. *Mon Weather Rev* 118(7):1483–1506
- Harris IC, Jones PD (2017) CRU TS4.00: climatic Research Unit (CRU) Time-Series (TS) version 4.00 of high-resolution gridded data of month-by-month variation in climate (Jan.1901–Dec.2015). Centre for Environmental Data Analysis, 25 August 2017. <https://doi.org/10.5285/edf8febfaad48abb2cbaf7d7e846a86>
- Hawkins E, Sutton R (2009) The potential to narrow uncertainty in regional climate predictions. *Bull Am Meteor Soc* 90(8):1095–1108
- Hawkins E, Sutton R (2011) The potential to narrow uncertainty in projections of regional precipitation change. *Clim Dyn* 37(1–2):407–418
- Hawkins E, Joshi M, Frame D (2014) Wetter then drier in some tropical areas. *Nat Clim Change* 4(8):646
- Hegerl G, Zwiers F (2011) Use of models in detection and attribution of climate change. *Wiley Interdiscip Rev Clim Change* 2(4):570–591. <https://doi.org/10.1002/wcc.121>
- Hirota N, Takayabu YN, Watanabe M et al (2011) Precipitation reproducibility over tropical oceans and its relationship to the double ITCZ problem in CMIP3 and MIROC5 climate models. *J Clim* 24(18):4859–4873. <https://doi.org/10.1175/2011JCLI14156.1>
- Hu Z, Zhang C, Hu Q et al (2014) Temperature changes in Central Asia from 1979 to 2011 based on multiple datasets. *J Clim* 27(3):1143–1167. <https://doi.org/10.1175/JCLI-D-13-00064.1>
- Hu Z, Li Q, Chen X et al (2016) Climate changes in temperature and precipitation extremes in an alpine grassland of Central Asia. *Theor Appl Climatol* 126(3–4):519–531. <https://doi.org/10.1007/s00704-015-1568-x>
- Hu Z, Zhou Q, Chen X et al (2017) Variations and changes of annual precipitation in Central Asia over the last century. *Int J Climatol* 37(S1):157–170. <https://doi.org/10.1002/joc.4988>
- Huang A, Zhou Y, Zhang Y et al (2014) Changes of the annual precipitation over central Asia in the twenty-first century projected by multimodels of CMIP5. *J Clim* 27(17):6627–6646. <https://doi.org/10.1175/JCLI-D-14-00070.1>
- Huang J, Yu H, Guan X, Wang G, Guo R (2015) Accelerated dryland expansion under climate change. *Nat Clim Change* 6(2):166–171. <https://doi.org/10.1038/nclimate2837>
- Huang J, Ji M, Xie Y, Wang S, He Y, Ran J (2016) Global semi-arid climate change over last 60 years. *Clim Dyn* 46(3–4):1131–1150. <https://doi.org/10.1007/s00382-015-2636-8>
- Huang J, Yu H, Dai A, Wei Y, Kang L (2017) Drylands face potential threat under 2 °C global warming target. *Nat Clim Change* 7(6):417–422. <https://doi.org/10.1038/nclimate3275>
- Intergovernmental Panel on Climate Change (IPCC) (2013) *Climate Change 2013: the physical science basis: Working group I contribution to the fifth assessment report of the Intergovernmental Panel on Climate Change*, edited by T. F. Stocker et al. Cambridge Univ Press, Cambridge
- James R, Washington R, Schleussner C et al (2017) Characterizing half-a-degree difference: a review of methods for identifying regional climate responses to global warming targets. *Wiley Interdiscip Rev Clim Change* 8(2):e457
- Jiang F, Hu RJ, Wang SP et al (2013) Trends of precipitation extremes during 1960–2008 in Xinjiang, the Northwest China. *Theor Appl Climatol* 111(1–2):133–148. <https://doi.org/10.1007/s00704-012-0657-3>
- King AD (2019) The drivers of nonlinear local temperature change under global warming. *Environ Res Lett* 14(6):064005. <https://doi.org/10.1088/1748-9326/ab1976>
- King AD, Karoly DJ (2017) Climate extremes in Europe at 1.5 and 2 degrees of global warming. *Environ Res Lett* 12(11):114031. <https://doi.org/10.1088/1748-9326/aa8e2c>
- King AD, Karoly DJ, Henley BJ (2017) Australian climate extremes at 1.5°C and 2°C of global warming. *Nat Clim Change* 7(6):412–416. <https://doi.org/10.1038/nclimate3296>
- Li Y, Huang JP, Ji MX, Ran JJ (2015) Dryland expansion in northern China from 1948 to 2008. *Adv Atmos Sci* 32(6):870–876. <https://doi.org/10.1007/s00376-014-4106-3>
- Li D, Zhou TJ, Zou LW, Zhang W, Zhang L (2018a) Extreme high-temperature events over East Asia in 1.5°C and 2°C warmer futures: analysis of NCAR CESM low-warming experiments. *Geophys Res Lett* 45(3):1541–1550. <https://doi.org/10.1002/2017GL076753>
- Li D, Zou L, Zhou T (2018b) Extreme climate event changes in China in the 1.5 and 2°C warmer climates: results from statistical and dynamical downscaling. *J Geophys Res Atmos* 123(18):10215–10230. <https://doi.org/10.1029/2018jd028835>
- Li W, Jiang Z, Zhang X, Li L, Sun Y (2018c) Additional risk in extreme precipitation in China from 1.5 °C to 2.0 °C global warming levels. *Sci Bull* 63(4):228–234. <https://doi.org/10.1016/j.scib.2017.12.021>
- Lin L, Wang Z, Yang Y, Zhang X, Zhang H, Dong W (2018) Additional intensification of seasonal heat and flooding extreme over China in a 2°C warmer world compared to 1.5°C. *Earths Future* 6:968–978. <https://doi.org/10.1029/2018ef000862>
- Nangombe S, Zhou T, Zhang W, Wu B, Hu S, Zou L, Li D (2018) Record-breaking climate extremes in Africa under stabilized 1.5 °C and 2 °C global warming scenarios. *Nat Clim Change* 8(5):375–380. <https://doi.org/10.1038/s41558-018-0145-6>
- Palazzi E, Filippi L, von Hardenberg J (2017) Insights into elevation-dependent warming in the Tibetan Plateau-Himalayas from CMIP5 model simulations. *Clim Dyn* 48(11–12):3991–4008. <https://doi.org/10.1007/s00382-016-3316-z>
- Pendergrass AG, Lehner F, Sanderson BM, Xu Y (2015) Does extreme precipitation intensity depend on the emissions scenario? *Geophys Res Lett* 42(20):8767–8774. <https://doi.org/10.1002/2015GL065854>
- Peng D, Zhou T (2017) Why was the arid and semiarid Northwest China getting wetter in the recent decades? *J Geophys Res Atmos* 122(17):9060–9075. <https://doi.org/10.1002/2016JD026424>
- Peng D, Zhou T, Zhang L, Wu B (2018) Human contribution to the increasing summer precipitation in Central Asia from 1961 to 2013. *J Clim* 31(19):8005–8021. <https://doi.org/10.1175/JCLI-D-17-0843.1>

- Peng D, Zhou T, Zhang L, Zou L (2019) Detecting human influence on the temperature changes in Central Asia. *Clim Dyn*. <https://doi.org/10.1007/s00382-019-04804-2>
- Sarojini B, Stott P, Black E (2016) Detection and attribution of human influence on regional precipitation. *Nat Clim Change* 6(7):669–675. <https://doi.org/10.1038/nclimate2976>
- Schleussner C, Lissner T, Fischer E et al (2016) Differential climate impacts for policy relevant limits to global warming: the case of 1.5 °C and 2 °C. *Earth Syst Dyn* 7:327–351. <https://doi.org/10.5194/esd-7-327-2016>
- Seneviratne SI, Donat MG, Pitman AJ et al (2016) Allowable CO<sub>2</sub> emissions based on regional and impact-related climate targets. *Nature* 529(7587):477. <https://doi.org/10.1038/nature16542>
- Shi Y, Shen Y, Kang E et al (2007) Recent and future climate change in northwest China. *Clim Change* 80(3–4):379–393. <https://doi.org/10.1007/s10584-006-9121-7>
- Shi C, Jiang Z, Chen W, Li L (2018) Changes in temperature extremes over China under 1.5 °C and 2 °C global warming targets. *Adv Clim Change Res* 9(2):120–129. <https://doi.org/10.1016/j.accre.2017.11.003>
- Sillmann J, Kharin VV, Zhang X, Zwiers FW, Bronaugh D (2013) Climate extremes indices in the CMIP5 multimodel ensemble: part 1. Model evaluation in the present climate. *J Geophys Res Atmos* 118(4):1716–1733
- Song F, Zhou T (2014) The climatology and interannual variability of East Asian summer monsoon in CMIP5 coupled models: does air-sea coupling improve the simulations? *J Clim* 27(23):8761–8777. <https://doi.org/10.1175/JCLI-D-14-00396.1>
- Stephens GL, Ecuyer LT, Forbes R, Gettleman A et al (2010) Dreary state of precipitation in global models. *J Geophys Res Atmos* 115(D24)
- Stott P, Gillett N, Hegerl G, Karoly D, Stone D, Zhang X, Zwiers F (2010) Detection and attribution of climate change: a regional perspective. *Wiley Interdiscip Rev Clim Change* 1(2):192–211
- Su F, Duan X, Chen D, Hao Z, Cuo L (2013) Evaluation of the global climate models in the CMIP5 over the Tibetan Plateau. *J Clim* 26(10):3187–3208. <https://doi.org/10.1175/JCLI-D-12-00321.1>
- Taylor KE (2001) Summarizing multiple aspects of model performance in a single diagram. *J Geophys Res Atmos* 106(D7):7183–7192. <https://doi.org/10.1029/2000JD900719>
- Taylor KE, Stouffer RJ, Meehl GA (2012) An overview of CMIP5 and the experiment design. *Bull Am Meteor Soc* 93(4):485–498. <https://doi.org/10.1175/BAMS-D-11-00094.1>
- Teutschbein C, Seibert J (2012) Bias correction of regional climate model simulations for hydrological climate-change impact studies: review and evaluation of different methods. *J Hydrol* 456:12–29
- Tiedtke M (1989) A comprehensive mass flux scheme for cumulus parameterization in large-scale models. *Mon Weather Rev* 117(8):1779–1800
- United Nations Framework Convention on Climate Change (UNFCCC) (2015) Adoption of the Paris Agreement. Report No. FCCC/CP/2015/L.9/Rev.1. <http://unfccc.int/resource/docs/2015/cop21/eng/l09r01.pdf>
- Wang Y, Zhou B, Qin D et al (2017) Changes in mean and extreme temperature and precipitation over the arid region of northwestern China: observation and projection. *Adv Atmos Sci* 34(3):289–305. <https://doi.org/10.1007/s00376-016-6160-5>
- Wang T, Miao JP, Sun JQ, Fu YH (2018) Intensified East Asian summer monsoon and associated precipitation mode shift under the 1.5 °C global warming target. *Adv Clim Change Res* 9(2):102–111. <https://doi.org/10.1016/j.accre.2017.12.002>
- Wartenburger R, Hirschi M, Donat MG et al (2017) Changes in regional climate extremes as a function of global mean temperature: an interactive plotting framework. *Geosci Model Dev* 10(9):3609–3634
- Weiland FS, van Beek L, Kwadijk J et al (2010) The ability of a GCM-forced hydrological model to reproduce global discharge variability. *Hydrol Earth Syst Sci* 14:1595–1621. <https://doi.org/10.5194/hess-14-1595-2010>
- Wu C, Huang G (2016) Projection of climate extremes in the Zhujiang River basin using a regional climate model. *Int J Climatol* 36(3):1184–1196
- Yang Y, Tang J, Wang S, Liu G (2018) Differential impacts of 1.5 °C and 2 °C warming on extreme events over China using statistically downscaled and bias-corrected CESM low-warming experiment. *Geophys Res Lett* 45(18):9852–9860. <https://doi.org/10.1029/2018gl079272>
- Yatagai A, Arakawa O, Kamiguchi K et al (2009) A 44-year daily gridded precipitation dataset for Asia based on a dense network of rain gauges. *Sola* 5:137–140. <https://doi.org/10.2151/sola.2009-035>
- Yatagai A, Kamiguchi K, Arakawa O et al (2012) APHRODITE: constructing a long-term daily gridded precipitation dataset for Asia based on a dense network of rain gauges. *Bull Am Meteor Soc* 93(9):1401–1415. <https://doi.org/10.1175/BAMS-D-11-00122.1>
- You Q, Jiang Z, Wang D, Pepin N, Kang S (2018) Simulation of temperature extremes in the Tibetan Plateau from CMIP5 models and comparison with gridded observations. *Clim Dyn* 51(1–2):355–369. <https://doi.org/10.1007/s00382-017-3928-y>
- Yu R, Zhai P, Lu Y (2018) Implications of differential effects between 1.5 and 2 °C global warming on temperature and precipitation extremes in China's urban agglomerations. *Int J Climatol* 38(5):2374–2385. <https://doi.org/10.1002/joc.5340>
- Zhang GJ, McFarlane NA (1995) Sensitivity of climate simulations to the parameterization of cumulus convection in the Canadian Climate Centre general circulation model. *Atmos Ocean* 33(3):407–446
- Zhang X, Alexander L, Hegerl GC et al (2011) Indices for monitoring changes in extremes based on daily temperature and precipitation data. *Wiley Interdiscip Rev Clim Change* 2(6):851–870. <https://doi.org/10.1002/wcc.147>
- Zhang W, Zhou T, Zhang L (2017) Wetting and greening Tibetan Plateau in early summer in recent decades. *J Geophys Res Atmos* 122(11):5808–5822. <https://doi.org/10.1002/2017JD026468>
- Zhang W, Zhou T, Zou L, Zhang L, Chen X (2018) Reduced exposure to extreme precipitation from 05 degrees C less warming in global land monsoon regions. *Nat Commun* 9(1):3153. <https://doi.org/10.1038/s41467-018-05633-3>
- Zhao C, Yao S, Liu J et al (2014) The spatial distribution of precipitation in northwest China. *J Electr Comput Eng* 1:1–5. <https://doi.org/10.1155/2014/514291>
- Zhou B, Zhai P, Chen Y, Yu R (2018a) Projected changes of thermal growing season over Northern Eurasia in a 1.5 °C and 2 °C warming world. *Environ Res Lett* 13(3):035004. <https://doi.org/10.1088/1748-9326/aaa6dc>
- Zhou T, Ren L, Liu H, Lu J (2018b) Impact of 1.5 °C and 2.0 °C global warming on aircraft takeoff performance in China. *Sci Bull* 63(11):700–707. <https://doi.org/10.1016/j.scib.2018.03.018>
- Zhou T, Sun N, Zhang W et al (2018c) When and how will the Millennium Silk Road witness 1.5 °C and 2 °C warmer worlds? *Atmos Ocean Sci Lett* 11(2):180–188. <https://doi.org/10.1080/16742834.2018.1440134>

**Publisher's Note** Springer Nature remains neutral with regard to jurisdictional claims in published maps and institutional affiliations.